Supplementary Information

Fatty acid carbon isotopes as indicators of palaeoproductivity in an Antarctic polynya environment

Kate Ashley[1], James Bendle[1], Xavier Crosta[2], Johan Etourneau[2,3], Philippine Campagne[2,4], Harry Gilchrist[1], Uthmaan Ibraheem[1], Sarah Greene[1], Sabine Schmidt[2], Yvette Eley[1], Guillaume Massé[4,5]

[1]School of Geography, Earth and Environmental Sciences, University of Birmingham, Edgbaston, Birmingham, B15 2TT, UK
[2]EPOC, UMR-CNRS 5805, Université de Bordeaux, 33615 Pessac, France
[3]Instituto Andaluz de Ciencias de la Tierra (CSIC), Avenida de las Palmeras 4, 18100 Armilla, Granada, Spain
[4]LOCEAN, UMR CNRS/UPCM/IRD/MNHN 7159, Université Pierre et Marie Curie, 4 Place Jussieu, 75252 Paris, France
[5]TAKUVIK, UMI 3376 UL/CNRS, Université Laval, 1045 avenue de la Médecine, Quebec City, Quebec, Canada G1V 0A6

S1. Core description and chronology

Sediment core DTGC2011 (66°24.50'S – 140°26.43'E, 1030 m water depth, 4.69 m gravity core) was recovered from the Dumont D'Urville Trough off the Adélie Land Coast, East Antarctica, aboard the R/V Astrolabe during the 2011 ALBION-HOLOCLIP cruise. The sediment is composed of diatom ooze and presents a laminated to banded structure throughout the entire sequence as revealed by positive X-ray images. The succession of dark and light laminations respectively represents the summer and spring seasons. High phytoplankton productivity during spring results in the deposition of greenish and light laminations while less organic-rich sedimentation during summer/autumn results in the preservation of dark and dense laminations (Maddison *et al.*, 2012).

The chronology of core DTGC2011 is based on radiocarbon dates and confirmed by ^{210}Pb excess activity measurements ($^{210}Pb_{xs}$; $T_{1/2}$ = 22,3 years) which is rapidly incorporated into the sediment from atmospheric fallout and water column scavenging. $^{210}Pb_{xs}$ analyses were performed on the first meter of core DTGC2011 until detection was too low to be representative (Fig S1b). The activities of ^{210}Pb and ^{226}Ra were measured on dried sediments by non-destructive gamma spectrometry using a well-type, high efficiency low-background detector equipped with a Cryo-cycle (CANBERRA). Activities are expressed in $mBq.g^{-1}$ and errors are based on 1 s.d. counting statistics (Fig. S1C). $^{210}Pb_{xs}$ was determined by subtracting the activity supported by its parent isotope, ^{226}Ra, from the total ^{210}Pb activity in the sediment. The $^{210}Pb_{xs}$ activity of ~160 $mBq.g^{-1}$ measured in DTGC2011 core-top is slightly lower than the activity of ~225 $mBq.g^{-1}$ measured in the first half-centimetre of the twin interface core DTCI2010, that preserved the interface (Campagne *et al.*, 2016). This suggests that core DTGC2011 lost the top few centimetres. By applying the decay law to the top $^{210}Pb_{xs}$ activities of each core, we estimate the age of the top DTGC2011 to be around 1997. The exponential decrease of sedimentary $^{210}Pb_{xs}$ activities in DTGC2011 was used to calculate a mean sedimentation accumulation rate of ~1.2 $cm.yr^{-1}$, by applying the constant flux / constant sedimentation (CF/CS) model . The deposition time (in years) was obtained by dividing the depth of each layer by the sediment accumulation rate and by assuming an age of 1997 at the top core. This yields a bottom age of ~1610 C.E. when linearly extrapolated over the whole core using the equation presented in Fig. 2B.

Acid insoluble organic matter (AIOM) radiocarbon dates were performed at five depths in core DTGC2011 and were complemented by one AIOM radiocarbon date in the core-top of the twin interface core DTCI2010 plus one AIOM radiocarbon date in a deep sediment trap moored at the same location and retrieved during the same cruise (Table 1). All dates were performed at the Center for Accelarator Mass Spectrometry from the Lawrence Livermore National Laboratory, USA. DTGC2011 core-top date was discarded due to a very large inversion value. DTGC2011 core-top age was therefore estimated from the dates obtained in DTCI2010 core-top and in the deep sediment trap, both of them providing a similar ^{14}C age of 1735 years for recently buried material. The raw dates were calibrated with CALIB7.02 software using the Marine 13 calibration curve (Reimer et al., 2013) after applying a total correction of 1625±100 years, which includes the local reservoir age of 1200±100 years (Ingølfsson et al., 1998) and the local dead carbon fraction of 425 years (Costa *et al.*, 2007 and references cited therein) as recommended for the area. This approach could not reconcile DTGC2011 core-top radiocarbon calibrated age with the $^{210}Pb_{xs}$ inferred age, suggesting that the dead carbon fraction of 425 years, averaged over Holocene sediment sequences, is not appropriate for the most recent sediments. An additional dead carbon fraction correction of 208 years was then applied to all calibrated dates. The depth-age conversion was achieved through a linear regression on the five control points (between 0 cm and 409 cm), therefore allowing to extrapolate ages down to 469 cm. As a result, core DTGC2011 spans the 1580-2000 C.E. period with a mean sedimentation rate of ~1 $cm.yr^{-1}$.

Both ^{14}C and $^{210}Pb_{xs}$ methods infer very similar depth-age relationships, with a maximum difference of thirty years at the core bottom. We chose to use the radiocarbon chronology as the ^{14}C approach provides a control over 409 cm as compare to 100 cm for the $^{210}Pb_{xs}$ approach.

Table S1: List of AMS 14C samples and detail of the calibration process to develop core DTGC2011 age model.

Provenance	Depth (cm)	Raw 14C age (years)	Reservoir age (years)	Calibrated age - 1 s (years B.P.)	Mean age (Years B.P.)	Mean age (Years C.E.)	Correction to 2010 (Years)	Final age (Years C.E.)
SED TRAP LOW		1735±35	1200±100	54-242	148	1802	208	2010
DTCI2010	0-0,5	1735±30	1200±100	54-242	148	1802	208	2010
DTGC2011	*0-0,5*	*8145±40*	*1200±100*	*7415-7595*				
DTGC2011	142-143	1835±35	1200±100	122-374	248	1702		1910
DTGC2011	204-205	2025±35	1200±100	321-505	413	1537		1745
DTGC2011	359-360	2070±30	1200±100	359-548	453,5	1496,5		1704,5
DTGC2011	409-410	2125±30	1200±100	440-614	527	1423		1631

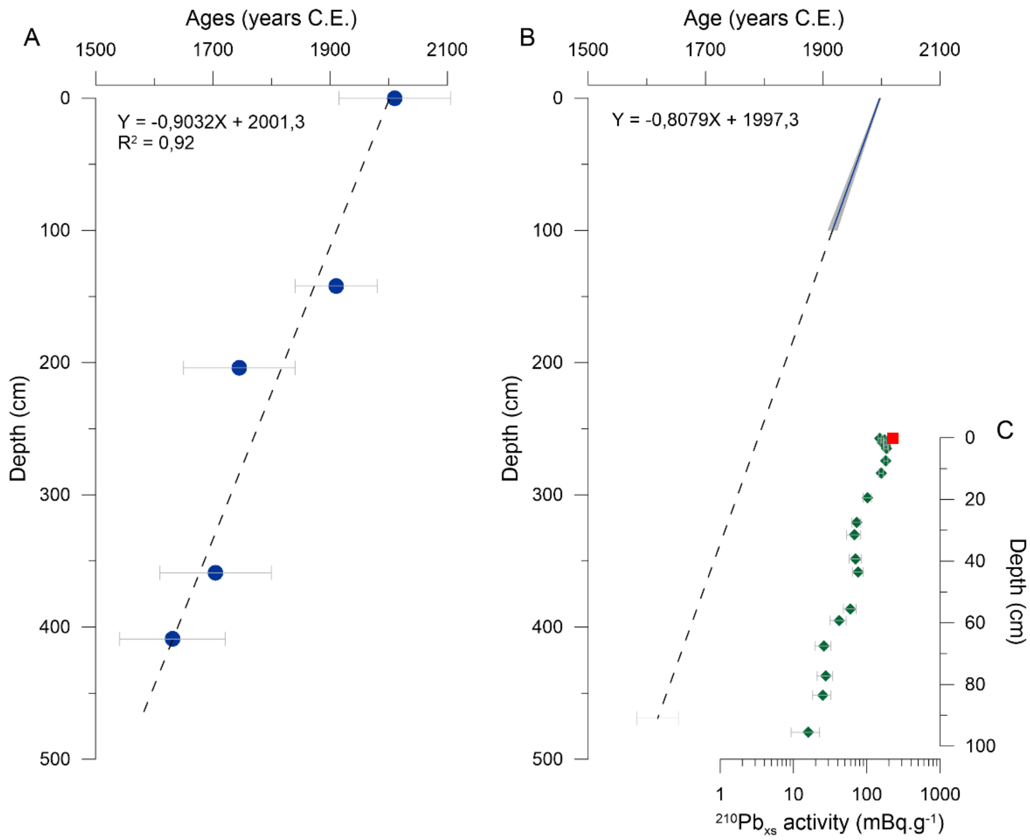

Figure S1: Chronology of core DTGC2011 based on AMS ^{14}C dates on AIOM, controlled by $^{210}Pb_{xs}$. (A) Corrected and calibrated ^{14}C mean ages in years C.E. (blue points) along with their 1 s range (horizontal bars) and the linear regression (dashed line) through the control points to extrapolate ages down to 469 cm. (B) $^{210}Pb_{xs}$ inferred ages in years C.E. over the first meter along with the 1 s error (grey envelope) and the linear regression (dashed line) through the first meter depth-age values to extrapolate ages down to 469 cm. (C) $^{210}Pb_{xs}$ activities in core DTGC2011 (green dots) and in the uppermost sample of the interface core DTCI2010 (red square) used to infer the sedimentation rate and ages over the first meter of the core.

S2. Fatty acid chromatography

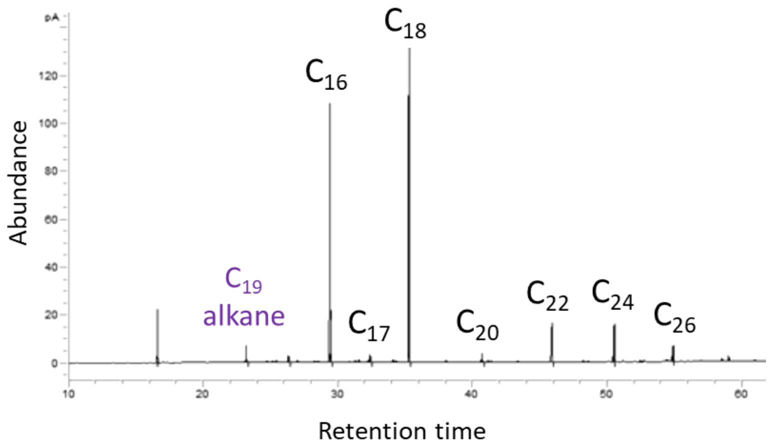

Figure S2: Typical chromatogram of the fatty acid fraction of DTGC2011 samples. Fatty acids are labelled according to their carbon number. An internal standard (C_{19} alkane), which was used for quantification of fatty acids, is labelled in purple.

S3. Sources of long-chain fatty acids

Table S2: Summary of several studies where long-chain fatty acids have been shown to be produced by aquatic organisms.

Study	Fatty Acids	Aquatic Contribution (%)	Location	Source
Naraoka and Ishiwatari (2000)	C_{20} - C_{30}	~ 38 (C30) - 88 (C20)	Northwest Pacific	Unknown
Holland et al. (2013)	C_{24} – C_{28}	n/a	Lake El'gygytgyn, Russia	Unknown
Volkman et al. (1980)	C_{24} – C_{28}	30 - 80	Victoria, Australia, intertidal	Diatoms
Schouten et al. (1998)	C_{28}	n/a	Culture	*Scenedesmus communis* (freshwater algae)
Yunker et al. (2005)	C_{20} – C_{28}	46 - 66	Arctic Ocean	Algae
Rogerson and Johns (1996)	C_{20} – C_{28}	100	Organic Lake, Antarctica (hypersaline, meromictic)	Bacteria
Lawson et al. (1986)	C_{24} – C_{30}	100	Westmere Reef, Auckland, New Zealand	*Halichondria moorei* (marine sponge)
Koopmans et al. (2014)	C_{24} – C_{30}	100	The Oosterschelde Estuary, Netherlands Lake Veere, Netherlands Northwest Mediterranean, Spain	*Haliclona oculta* and Haliclona *xena* (marine sponges) *Halichondria panacea* and *Haliclona xena* (marine sponges) *Dysidea avara* and *Aplysina aerophoba* (marine sponges)
Viso et al. (1993)	C_{22} – C_{34}	100	Mediterranean coasts of France and Greece	*Posidonia oceanica* (seagrass)
Leblond and Chapman (2000)	C_{20} – C_{22}, trace C_{24}	100	Culture	Various dinoflagellate species

References

Campagne, P., et al. (2016) Sedimentary response to sea ice and atmospheric variability over the instrumental period off Adélie Land, East Antarctica, *Biogeosciences*, 13(14), pp. 4205–4218. doi: 10.5194/bg-13-4205-2016.

Costa, E., Dunbar, R. B., Kryc, K.A. et al. (2007) Solar forcing and El Nino-Southern Oscillation (ENSO) influences on productivity cycles interpreted from a late-Holocene high-resolution marine sediment record, Adélie Drift, East Antarctic margin', Open-File Report - U. S. Geological Survey, p. Short Research Paper 036. doi: 10.3133/of2007-1047.srp036.

Holland, A.R., Petsch, S.T., Castañeda, I.S., et al. (2013) A biomarker record of Lake El'gygytgyn, Far East Russian arctic: Investigating sources of organic matter and carbon cycling during marine isotope stages 1-3. *Climate of the Past*, 9 (1): 243–260. doi:10.5194/cp-9-243-2013.

Ingólfsson, Ó, Hjort, C., Berkman, P., Björck, S., Colhoun, E., Goodwin, I., et al. (1998). Antarctic glacial history since the Last Glacial Maximum: An overview of the record on land. Antarctic Science, 10(3), 326-344. doi:10.1017/S095410209800039X

Koopmans, M., van Rijswijk, P., Boschker, H.T.S., et al. (2014) Seasonal Variation of Fatty Acids and Stable Carbon Isotopes in Sponges as Indicators for Nutrition: Biomarkers in Sponges Identified. *Marine Biotechnology*, 17 (1): 43–54. doi:10.1007/s10126-014-9594-8.

Lawson, M.P., Bergquist, P.R. and Cambie, R.C. (1986) The cellular localization of long chain fatty acids in sponges. *Tissue and Cell*, 18 (1): 19–26. doi:10.1016/0040-8166(86)90004-2.

Leblond, J.D. and Chapman, P.J. (2000) LIPID CLASS DISTRIBUTION OF HIGHLY UNSATURATED LONG CHAIN FATTY ACIDS IN MARINE DINOFLAGELLATES. *Journal of Phycology*, 36: 1103–1108.

Maddison, E. J., Pike, J. and Dunbar, R. (2012) 'Seasonally laminated diatom-rich sediments from Dumont d'Urville Trough, East Antarctic Margin: Late-Holocene Neoglacial sea-ice conditions', The Holocene, 22(8), pp. 857–875. doi: 10.1177/0959683611434223.

Naraoka, H. and Ishiwatari, R. (2000) Molecular and isotopic abundances of long-chain n-fatty acids in open marine sediments of the western North Pacific. *Chemical Geology*, 165 (1–2): 23–36. doi:10.1016/S0009-2541(99)00159-X.

Rogerson, J.H. and Johns, R.B. (1996) "A geolipid characterization of Organic Lake - A hypersaline meromictic Antarctic lake." In *Organic Geochemistry*. 1996. pp. 1–8. doi:10.1016/S0146-6380(96)00109-X.

Schouten, S., Klein Breteler, W.C.., Blokker, P., et al. (1998) Biosynthetic effects on the stable carbon isotopic compositions of algal lipids: implications for deciphering the carbon isotopic biomarker record. *Geochimica et Cosmochimica Acta*, 62 (8): 1397–1406. doi:10.1016/S0016-7037(98)00076-3.

Viso, A.-C., Pesando, D., Bernard, P., et al. (1993) Lipid components of the mediterranean seagrass Posidonia Oceanica. *Phytochemistry*, 34 (2): 381–387. doi:10.1016/0031-9422(93)80012-H.

Volkman, J.K., Eglinton, G. and Corner, E.D.S. (1980) Sterols and fatty acids of the marine diatom biddulphia sinensis. *Phytochemistry*, 19 (8): 1809–1813. doi:10.1016/S0031-9422(00)83818-2.

Yunker, M.B., Belicka, L.L., Harvey, H.R., et al. (2005) Tracing the inputs and fate of marine and terrigenous organic matter in Arctic Ocean sediments: A multivariate analysis of lipid biomarkers. *Deep-Sea Research Part II: Topical Studies in Oceanography*, 52 (24–26): 3478–3508. doi:10.1016/j.dsr2.2005.09.008.